Synthesis of Me_2Si-Bridged *ansa*-Zirconocenes by Amine Elimination

Gary M. Diamond and Richard F. Jordan*

Department of Chemistry, University of Iowa, Iowa City, Iowa 52242

Jeffrey L. Petersen

Department of Chemistry, West Virginia University, Morgantown, West Virginia 26506

Received February 13, 1996[⊗]

Me_2Si-bridged *ansa*-zirconocenes of interest for α-olefin polymerization catalysis are prepared in good yield by amine elimination reactions. The reaction of $Me_2Si(1\text{-}C_5H_4\text{-}3\text{-}^tBu)_2$ (**3**) and $Zr(NMe_2)_4$ affords $Me_2Si(1\text{-}C_5H_3\text{-}3\text{-}^tBu)_2Zr(NMe_2)_2$ (**4**) in 95% NMR yield (*rac*/*meso* = 1/2) and pure *meso*-**4** in 38% isolated yield. The reaction of $Me_2Si(1\text{-}C_5H_3\text{-}2\text{-}Me\text{-}4\text{-}^tBu)_2$ (**6**) with $Zr(NMe_2)_4$ affords $Me_2Si(1\text{-}C_5H_2\text{-}2\text{-}Me\text{-}4\text{-}^tBu)_2Zr(NMe_2)_2$ (**7**) in 90% NMR yield (*rac*/*meso* = 2.5/1) and pure *rac*-**7** in 52% isolated yield. The 1/2 *rac*-**4**/*meso*-**4** and 2.5/1 *rac*-**7**/*meso*-**7** ratios are the thermodynamic ratios, and the *rac*/*meso* isomerizations are catalyzed by NMe_2H via reversible Zr−Cp bond aminolysis. The thermodynamic bias for *meso*-**4** is ascribed to the ease of distortion of the metallocene framework of this diastereomer by a lateral deformation which reduces steric crowding between the amide ligands and the Cp substituents. The reaction of **6** and $Zr(NEt_2)_4$ proceeds only in 1,2-dichlorobenzene at 180 °C, affording $Me_2Si(1\text{-}C_5H_2\text{-}2\text{-}Me\text{-}4\text{-}^tBu)_2ZrCl_2$ (*rac*-**1**) in 35% NMR yield (*rac*/*meso* = 3/1). The reaction of **6** and the piperidide complex $Zr(NC_5H_{10})_4$ (*m*-xylene, 140 °C, 24 h) affords *rac*-$Me_2Si(1\text{-}C_5H_2\text{-}2\text{-}Me\text{-}4\text{-}^tBu)_2Zr(NC_5H_{10})_2$ (*rac*-**9**) in 35% NMR yield (no *meso* detected) and pure *rac*-**9** in 7% isolated yield. The reaction of **6** and the pyrrolidide complex $Zr(NC_4H_8)_4$ (*m*-xylene, 90 °C, 4h) affords $Me_2Si(1\text{-}C_5H_2\text{-}2\text{-}Me\text{-}4\text{-}^tBu)_2Zr(NC_4H_8)_2$ (**10**) in 80% NMR yield (*rac*/*meso* = 3/1) and pure *rac*-**10** in 39% isolated yield. The molecular structure of *rac*-**10** was determined by X-ray crystallography and exhibits severe crowding between the amide ligands and the Cp substituents. Treatment of *rac*-**7** or *rac*-**10** with Me_3SiCl results in clean conversion to *rac*-**1** without isomerization.

Introduction

The most promising *ansa*-metallocene catalysts for the isospecific polymerization of α-olefins contain R_2Si bridged bis(cyclopentadienyl) or bis(indenyl) ligands.[1,2] Brintzinger and Rieger have reported that activation of the C_2-symmetric metallocene *rac*-$Me_2Si(1\text{-}C_5H_2\text{-}2\text{-}Me\text{-}4\text{-}^tBu)_2ZrCl_2$ (*rac*-**1**, Chart 1) with methylalumoxane (MAO) yields a highly isoselective propylene polymerization catalyst.[3,4] The α- and β-Cp substituents (i.e. the substituents at the 2 and 4 positions versus the bridge) are critical for catalyst performance. Replacement of the β-^{t}Bu substituents with ^{i}Pr groups results in increased activity but decreased isoselectivity.[3] Also, under the same conditions (50 °C, toluene, 2 atm propylene, Al/Zr = 300/1), *rac*-**1** produces polypropylene with much higher molecular weight and isotacticity, and fewer regioirregularities, than do *rac*-$Me_2Si(1\text{-}C_5H_3\text{-}3\text{-}^tBu)_2ZrCl_2$ (*rac*-**2**, Chart 1) and *rac*-(EBTHI)$ZrCl_2$ (EBTHI = ethylene-1,2-bis(1-tetrahydroindenyl)).[3] Spaleck has reported similar bridge and substituent effects for *ansa*-metallocenes with Me_2Si-bridged bis(indenyl) ligands.[2b,c]

Chart 1

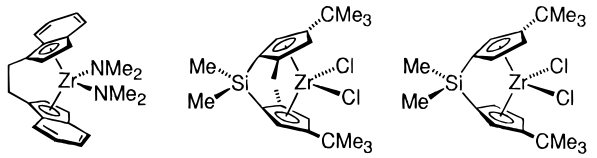

rac-(EBI)$Zr(NMe_2)_2$ *rac*-**1** *rac*-**2**

Brintzinger prepared **1** in 15% yield in a *rac*/*meso* ratio of 2/1 by the reaction of $Me_2Si(1\text{-}C_5H_2\text{-}2\text{-}Me\text{-}4\text{-}^tBu)_2K_2$ and $ZrCl_4(THF)_2$.[5] Pure *rac*-**1** was obtained only after repeated recrystallization, in 9% yield.[6] Following a similar procedure, Brintzinger prepared **2** in 19% yield in a *rac*/*meso* ratio of 1/1 and obtained pure *rac*-**2** in 7% yield after repeated recrystallization.[5] By employing $Me_2Si(1\text{-}C_5H_2\text{-}3\text{-}^tBu)_2Li_2$, Mise obtained **2** in 33% yield

[⊗] Abstract published in *Advance ACS Abstracts,* August 15, 1996.

(1) Reviews (a) Thayer, A. M. *Chem. Eng. News* **1995**, *73* (37), 15. (b) Brintzinger, H. H.; Fischer, D.; Mülhaupt, R.; Rieger, B.; Waymouth, R. M. *Angew. Chem., Int. Ed. Engl.* **1995**, *34*, 1143. (c) Sinclair, K. B.; Wilson, R. B. *Chem. Ind.* **1994**, 857. (d) Möhring, P. C.; Coville, N. J. *J. Organomet. Chem.* **1994**, *479*, 1. (e) Horton, A. D. *Trends Polym. Sci.* **1994**, *2*, 158.

(2) (a) Stehling, U.; Diebold, J.; Kirsten, R.; Roll, W.; Brintzinger, H. H.; Jungling, S.; Mülhaupt, R.; Langhauser, F. *Organometallics* **1994**, *13*, 964. (b) Spaleck, W.; Kuber, F.; Winter, A.; Rohrmann, J.; Bachmann, B.; Antberg, M.; Dolle, V.; Paulus, E. F. *Organometallics* **1994**, *13*, 954. (c) Spaleck, W.; Antberg, M.; Rohrmann, J.; Winter, A.; Bachmann, B.; Kiprof, P.; Behm, J.; Herrmann, W. A. *Angew. Chem., Int. Ed. Engl.* **1992**, *31*, 1347. (d) Chacon, S. T.; Coughlin, E. B.; Henling, L. M.; Bercaw, J. E. *J. Organomet. Chem.* **1995**, *497*, 171.

(3) Roll, W.; Brintzinger, H. H.; Rieger, B.; Zolk, R. *Angew. Chem., Int. Ed. Engl.* **1990**, *29*, 279.

(4) Rieger, B.; Reinmuth, A.; Roll, W.; Brintzinger, H. H. *J. Mol. Catal.* **1993**, *82*, 67.

(5) Wiesenfeldt, H.; Reinmuth, A.; Barsties, E.; Evertz, K.; Brintzinger, H. H. *J. Organomet. Chem.* **1989**, *369*, 359.

(6) Reinmuth, A. Ph.D. Dissertation, University of Konstanz, 1992.

S0276-7333(96)00105-7 CCC: $12.00

as a 1/1 mixture of *rac* and *meso* isomers; recrystallization from toluene provided a 2.7/1 *rac*/*meso* mixture.[7] Salt elimination syntheses of other *ansa*-metallocenes with Me_2Si-bridged bis(cyclopentadienyl) ligands typically provide the pure *rac* product in only 5−10% yield, and separation from the undesired *meso* isomer is not always possible.[2−7]

We recently reported that the amine elimination reaction of $(EBI)H_2$ (1,2-bis(3-indenyl)ethane) and $Zr(NMe_2)_4$ provides an efficient stereoselective route to *rac*-$(EBI)Zr(NMe_2)_2$ (EBI = ethylene-1,2-bis(1-indenyl), Chart 1).[8] We also showed that *rac*-$(EBI)Zr(NMe_2)_2$ is cleanly converted to *rac*-$(EBI)ZrCl_2$ (2 equiv of $[NMe_2H_2]Cl$ or Me_3SiCl), or *rac*-$(EBI)ZrMe_2$ (4 equiv $AlMe_3$),[8] and can be activated for α-olefin polymerization via in situ alkylation with AlR_3 reagents and subsequent treatment with MAO or cationic activators ($[Ph_3C][B(C_6F_5)_4]$ or $[R_3NH][B(C_6F_5)_4]$).[9] *rac*-$(EBI)ZrX_2$ compounds can be prepared using other Zr amides (e.g. $Zr(NEt_2)_4$, $Zr(NMe_2)_2(N^iPr_2)_2$, $Zr(NC_4H_8)_4$); however the steric bulk of the amides is crucial in determining the products obtained and the reaction conditions required, and the optimum amide starting material is $Zr(NMe_2)_4$.[10] Here we describe extension of the amine elimination approach to the synthesis of *ansa*-metallocenes with Me_2Si-bridged bis(cyclopentadienyl) ligands. The synthesis of *rac*-$Me_2Si(indenyl)_2ZrX_2$ complexes by amine elimination is described in another paper in this series.[11]

Results and Discussion

Synthesis of *meso*-$Me_2Si(1\text{-}C_5H_3\text{-}3\text{-}^tBu)_2Zr(NMe_2)_2$ (*meso*-4). The amine elimination reaction of $Me_2Si(C_5H_4\text{-}3\text{-}^tBu)_2$ (**3**) and $Zr(NMe_2)_4$ was initially studied under the reaction conditions employed for the synthesis of *rac*-$(EBI)Zr(NMe_2)_2$ (toluene, 100 °C, 17 h, evolved NMe_2H allowed to escape via an oil bubbler).[8] Under these conditions, the metallocene bis(amide) complex $Me_2Si(1\text{-}C_5H_3\text{-}3\text{-}^tBu)_2Zr(NMe_2)_2$ (**4**) is formed in 95% NMR yield in a *rac*/*meso* ratio of 1/2 (eq 1). Recrystallization from hexane gives pure *meso*-**4**, a yellow crystalline solid, in 38% isolated yield.

Further studies of this system provide insight to the mechanism of metallocene formation in eq 1. The reaction of **3** and $Zr(NMe_2)_4$ at lower temperatures yields slightly lower *rac*/*meso* product ratios. For example, in *m*-xylene at 23 °C for 2 h (system open to oil bubbler), **4** is formed in 95% NMR yield in a *rac*/*meso* ratio of 1/1.5. In the absence of added amine, pure *meso*-**4** is configurationally stable in C_6D_6 at 23 °C. However, when 1 equiv of NMe_2H is added, isomerization occurs and a 1/2 *rac*-**4**/*meso*-**4** ratio is obtained in less than 2 h; this ratio does not change further after 14 h at 23 °C. As both experiments were conducted under the same lighting conditions (normal room light),

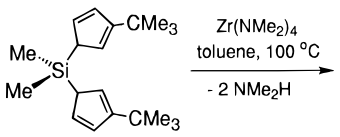

3

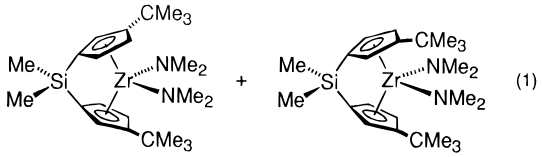

rac-**4** / *meso*-**4**

ratio: 1 / 2

the isomerization is not due to photoisomerization.[12] These observations establish that (i) the thermodynamic *rac*-**4**/*meso*-**4** ratio is 1/2, (ii) the kinetic product ratio of eq 1 is somewhat higher, and (iii) the *rac*-**4**/*meso*-**4** isomerization is catalyzed by NMe_2H. As illustrated in Scheme 1, the isomerization most likely occurs via mono(cyclopentadienyl) intermediate **5**, which however, was not observed. This isomerization mechanism is analogous to that established earlier for $(EBI)Zr(NMe_2)_2$ and $Me_2Si(indenyl)_2Zr(NMe_2)_2$.[8,11]

Comparison of Amine Elimination Syntheses of 4 and $(EBI)Zr(NMe_2)_2$. The amine elimination and aminolysis reactions which form and interconvert **5** and **4** (Scheme 1) are much faster than the corresponding reactions in the $(EBI)Zr(NMe_2)_2$ system. As noted above, at 23 °C the reaction of **3** with $Zr(NMe_2)_4$ results in complete formation of **4** in 2 h without buildup of **5**, and the reaction of *meso*-**4** with 1 equiv of NMe_2H results in isomerization to the thermodynamic 1/2 *rac*/*meso* mixture within 2 h. In contrast, the reaction of $(EBI)H_2$ and $Zr(NMe_2)_4$ under the same conditions yields a mixture of 10% $(EBI)Zr(NMe_2)_2$ and 90% mono(indenyl) species $(\eta^5\text{-}C_9H_6CH_2CH_2C_9H_7)Zr(NMe_2)_3$ and $(\mu\text{-}\eta^5,\eta^5\text{-EBI})\{Zr(NMe_2)_3\}_2$ after 14 h.[8b] Also, when 2 equiv of NMe_2H is added to a 1/1 *rac*-*meso* $(EBI)Zr(NMe_2)_2$ mixture at 23 °C, the *meso* isomer is very slowly (>100 h) converted to $(\eta^5\text{-}C_9H_6CH_2CH_2C_9H_7)Zr(NMe_2)_3$ and $(\mu\text{-}\eta^5,\eta^5\text{-EBI})\{Zr(NMe_2)_3\}_2$, and the *rac* isomer does not react.[8b]

The acidities of **3** and the pendant cyclopentadiene in **5** are likely to be similar to that of cyclopentadiene (pK_a in Me_2SO = 18.0), because the effects of alkyl and silyl groups on pK_a values are similar but opposite, and thus will tend to cancel out.[13,14] Thus **3** and the pendant cyclopentadiene in **5** are significantly more acidic than $(EBI)H_2$ and the pendant indene of $(\eta^5\text{-}C_9H_6CH_2CH_2C_9H_7)Zr(NMe_2)_3$ (cf. pK_a of 3-methylindene in Me_2SO = 22.5),[14] and the amine eliminations leading to **5** and **4** are thus expected to be faster than the analogous reactions in the EBI system. The aminolysis of the metallocenes back to the mono(cyclopentadienyl) intermediates (e.g. **4** + NMe_2H → **5** in Scheme 1) likely

(7) Mise, T.; Miya, S.; Yamazaki, H *Chem. Lett.* **1989**, 1853.
(8) (a) Diamond, G. M.; Rodewald, S.; Jordan, R. F. *Organometallics* **1995**, *14*, 5. (b) Diamond, G. M.; Jordan, R. F.; Petersen, J. L. *J. Am. Chem. Soc.*, in press.
(9) Kim, I.; Jordan, R. F. *Macromolecules* **1996**, *29*, 489.
(10) Diamond, G. M.; Jordan, R. F.; Petersen, J. L. *Organometallics* **1996**, *15*, 4030.
(11) Christopher, J. N.; Diamond, G. M.; Jordan, R. F.; Petersen, J. L. *Organometallics* **1996**, *15*, 4038.
(12) For photoisomerization of *ansa*-metallocenes see: (a) Wild, F. R. W. P.; Zsolnai, L.; Huttner, G.; Brintzinger, H. H. *J. Organomet. Chem.* **1982**, *232*, 233. (b) Rheingold, A. L.; Robinson, N. P.; Whelan, J.; Bosnich, B. *Organometallics* **1992**, *11*, 1869. (c) Collins, S.; Hong, Y.; Ramachandran, R.; Taylor, N. J. *Organometallics* **1991**, *10*, 2349. (d) Collins, S.; Hong, Y.; Taylor, N. J. *Organometallics* **1990**, *9*, 2695.
(13) Bordwell, F. G.; Bausch, M. J. *J. Am. Chem. Soc.* **1983**, *105*, 6188.
(14) Bordwell, F. G. *Acc. Chem. Res.* **1988**, *21*, 456.

Scheme 1

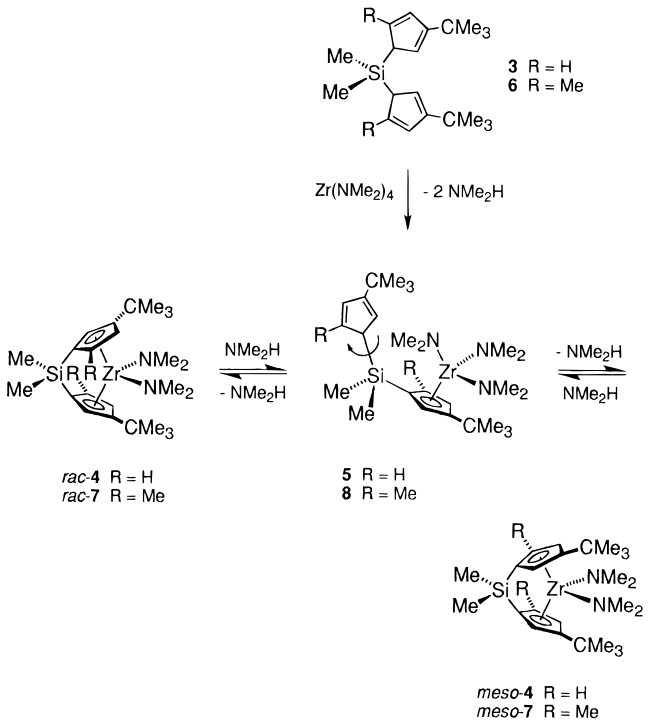

proceeds by initial coordination of NMe_2H and subsequent proton transfer to a cyclopentadienyl carbon, as illustrated generically in eq 2 (X = bridge). The lower

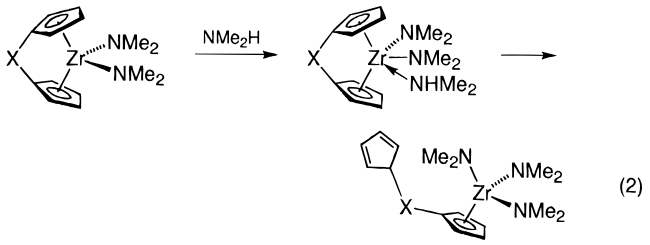

basicity of the cyclopentadienyl ligands in **4** (versus the indenyl ligands in (EBI)Zr(NMe_2)$_2$) may result in a more electrophilic metal center and a greater preference for NMe_2H coordination compared to (EBI)Zr(NMe_2)$_2$.[15] Additionally, if the departing cyclopentadiene develops significant carbanionic (Cp^-) character in the proton transfer transition state, then factors that decrease CpH acidity would destabilize the transition state and slow the reaction. Decreased crowding in **3** versus (EBI)H_2 may also contribute to the reactivity differences.

The stereochemical properties of **4** and (EBI)Zr(NMe_2)$_2$ are quite different: the thermodynamic *rac*/*meso* ratio is 1/2 for **4** but >20/1 for (EBI)Zr(NMe_2)$_2$.[8] Earlier we proposed that *meso*-(EBI)Zr(NMe_2)$_2$ is disfavored by steric crowding between the NMe_2 and EBI ligands, which is particularly severe due to the proximity of one amide ligand to both six-membered EBI rings. Similar steric crowding might be expected between one

Chart 2

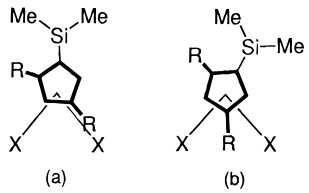

of the $-NMe_2$ ligands and the β-^{t}Bu substituents in *meso*-**4**. However, it is likely that steric crowding is relieved in *meso*-**4** by "lateral deformation", i.e. rotation of the bis(cyclopentadienyl) ligand away from axial alignment with the amide ligands (Chart 2a), to a conformation in which the β-Cp substituents lie between the amide ligands (Chart 2b). Brintzinger has reported lateral deformations of this type in several *ansa*-metallocenes and has proposed that they relieve steric interactions between the equatorial ligands and β-Cp substituents.[16] This stabilization effect is most important in the *meso* isomers and may provide a thermodynamic bias for the *meso* over the *rac* isomers in some cases. Lateral deformation in a *rac* structure forces one β-substituent into the narrow region of the metallocene wedge; in contrast lateral deformation in a *meso* structure positions both β-substituents in the more open frontal region of the wedge. Brintzinger's analysis of intramolecular van der Waals repulsions in *ansa*-metallocenes indicates that lateral deformations are favored by β-Cp substituents but strongly disfavored by α-Cp substituents, which are forced into the narrow region of the metallocene wedge in the distorted structure (Chart 2b).

For example, *meso*-(Me_2C)$_2$(1-C_5H_3-3-$SiMe_3$)$_2$$TiCl_2$ shows significant lateral deformation, such that both $SiMe_3$ groups occupy central positions between the Cl atoms.[17] This reduces the steric crowding between the $SiMe_3$ groups and Cl atoms, such that the $SiMe_3$ groups are bent out of the Cp plane by only 7−9°. In contrast, the structures of *rac*-(Me_2C)$_2$(1-C_5H_3-3-$SiMe_3$)$_2$$TiMe_2$ and *rac*-(Me_2C)$_2$(1-C_5H_3-3-^{t}Bu)$_2$$ZrCl_2$ show no lateral deformation, and the β-substituents are bent out of the Cp plane by 10−12°.[17] More relevant to the problem at hand, *meso*-Me_2Si(1-C_5H_3-3-^{t}Bu)$_2$$ZrCl_2$ (*meso*-**2**), the dichloride analogue of *meso*-**4**, exhibits a large lateral deformation (dihedral angle between centroid−Si−centroid and centroid−Zr−centroid planes = 17.9°).[18] In contrast, *meso*-(EBI)$ZrCl_2$, the dichloride analogue of *meso*-(EBI)Zr(NMe_2)$_2$, exhibits a much smaller lateral deformation (2°),[19] due to the α-substituents (i.e. fused benzo rings of the indenyl ligands) and perhaps the different bridge structure. By analogy, a significant lateral deformation is expected for and may stabilize *meso*-**4**, but not *meso*-(EBI)Zr(NMe_2)$_2$, and a lower *rac*/*meso* ratio is therefore expected for **4** versus (EBI)Zr-

(15) For studies of the influence of Cp substituents and bridge structures on the electrophilicity of zirconocene complexes see: (a) Alameddin, N. G.; Ryan, M. F.; Eyler, J. R.; Siedle, A. R.; Richardson, D. E. *Organometallics* **1995**, *14*, 5005. (b) Bajgur, C. S.; Tikkanen, W. R.; Petersen, J. L. *Inorg. Chem.* **1985**, *24*, 2539. (c) Woo, T. K.; Fan, L.; Ziegler, T. *Organometallics* **1994**, *13*, 2252. (d) Siedle, A. R.; Newmark, R. A.; Lamanna, W. M.; Schroepfer, J. N. *Polyhedron* **1990**, *9*, 301. (e) Gassman, P. G.; Deck, P. A.; Winter, C. H.; Dobbs, D. A.; Cao, D. H. *Organometallics* **1992**, *11*, 959.

(16) (a) Burger, P.; Hortmann, K.; Brintzinger, H. H. *Makromol. Chem., Makromol. Symp.* **1993**, *66*, 127. (b) Burger, P.; Diebold, J.; Guttmann, S.; Hund, H. U.; Brintzinger, H. H. *Organometallics* **1992**, *11*, 1319.

(17) Guttmann, S.; Burger, P.; Hund, H. U.; Hofmann, J.; Brintzinger, H. H. *J. Organomet. Chem.* **1989**, *369*, 343.

(18) (a) Schmidt, K.; Diplomarbiet Thesis, University of Konstanz, 1994. (b) The β-^{t}Bu groups of *meso*-**2** are bent 8° out of Cp plane, compared with 10° for *rac*-**1**, which shows no lateral deformation.

(19) The dihedral angle between the centroid−(CH_2−CH_2 bridge midpoint)−centroid and centroid−Zr−centroid planes in *meso*-(EBI)-$ZrCl_2$ is 2° as calculated from data reported in: Piemontesi, F.; Camurati, I.; Resconi, L.; Balboni, D.; Sironi, A.; Moret, M.; Ziegler, R.; Piccolrovazzi, N. *Organometallics* **1995**, *14*, 1256.

$(NMe_2)_2$. In a similar vein, Marks has proposed that lateral deformation may account for the preference shown by some sterically crowded C_1-symmetric chiral lanthanide *ansa*-metallocenes for pseudo-*meso* rather than pseudo-*rac* configurations.[20]

Synthesis of *rac*-$Me_2Si(1\text{-}C_5H_2\text{-}2\text{-}Me\text{-}4\text{-}^tBu)_2Zr(NMe_2)_2$ (*rac*-7). Several groups have shown that the cyclopentadienyl ring substituents have a significant effect on the yield and stereoselectivity of salt elimination syntheses of *ansa*-metallocenes and, in particular, that the *rac*/*meso* product ratio can be significantly increased by introducing substituents at the α-position (adjacent to the bridge).[2d,5] This is fortunate because α-substituents also have a beneficial effect on catalyst performance, as noted above. For example Brintzinger reported a higher *rac*/*meso* ratio in the salt elimination synthesis of $Me_2Si(1\text{-}C_5H_2\text{-}2\text{-}Me\text{-}4\text{-}^tBu)_2ZrCl_2$ (**1**, *rac*/*meso* = 2/1) compared with $Me_2Si(1\text{-}C_5H_3\text{-}3\text{-}^tBu)_2ZrCl_2$ (**2**, *rac*/*meso* = 1/1);[5] it was proposed that the stereoselectivity of these reactions is under primarily kinetic control, and the preference for *rac*-**1** is due to unfavorable steric repulsions between the α-methyl substituents in the transition state leading to *meso*-**1**. Accordingly, we investigated the effect of α-substitution on amine elimination syntheses of *ansa*-metallocenes.

The reaction of $Me_2Si(1\text{-}C_5H_3\text{-}2\text{-}Me\text{-}4\text{-}^tBu)_2$ (**6**) with $Zr(NMe_2)_4$ in toluene at 100 °C for 5 h (system open to oil bubbler) affords the desired *ansa*-zirconocene $Me_2Si(1\text{-}C_5H_2\text{-}2\text{-}Me\text{-}4\text{-}^tBu)_2Zr(NMe_2)_2$ (**7**) in 90% NMR yield in a *rac*/*meso* ratio of 2.5/1 (eq 3). Recrystallization from

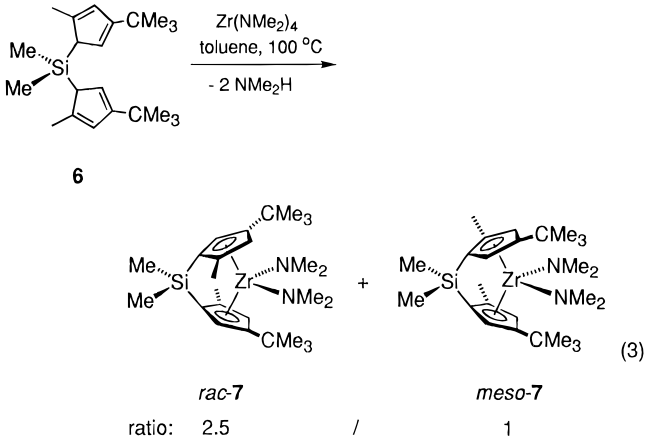

hexane gives pure *rac*-**7**, a yellow crystalline solid, in 52% isolated yield. The use of a longer reaction time (17 h) has no effect on the yield or stereoselectivity.[21]

The reaction of **6** with $Zr(NMe_2)_4$ in C_6D_6 at lower temperatures was monitored by ^1H NMR spectroscopy. After 1 h at 60 °C, **7** was formed in 25% yield in a *rac*/*meso* ratio of 6/1. After a further 2 h at 60 °C the reaction was 70% complete and the *rac*/*meso* ratio had decreased to 2.5/1. After a further 14 h at 85 °C, the reaction was complete and the *rac*-**7**/*meso*-**7** ratio remained 2.5/1. In the absence of added amine, pure *rac*-**7** is configurationally stable in C_6D_6 at 100 °C; no *meso*-**7** is formed even after 18 h. However, when *rac*-**7** was heated (100 °C) in the presence of 2 equiv of NMe_2H in C_6D_6, a 2.8/1 *rac*-**7**/*meso*-**7** mixture was obtained after 30 min; the *rac*/*meso* ratio decreased to 2.5/1 after 2 h and did not change further after 15 h.

These observations indicate that (i) *rac*-**7** is the kinetic product of eq 3, (ii) the thermodynamic *rac*-**7**/*meso*-**7** ratio is 2.5/1, and (iii) the *rac*-**7**/*meso*-**7** epimerization is catalyzed by NMe_2H via the process shown in Scheme 1. As for **4** but in contrast to the synthesis of (EBI)$Zr(NMe_2)_2$, the presumed mono-Cp intermediate species **8** was not observed in the synthesis or isomerization of **7**. This implies that the intramolecular amine elimination of **8** to **7** is faster than the formation of **8** from **6** and $Zr(NMe_2)_4$ under the conditions studied.

The rates of formation and isomerization of **7** are both slower than for **4**, which lacks the α-Me Cp substituents. This difference reflects the decreased acidity and increased steric crowding of **6** and its derivatives relative to **3** and its derivatives due to the α-methyl substituents. The 5-fold increase in the thermodynamic *rac*/*meso* ratio resulting from incorporation of the α-Me substituents (2.5/1 for **7** vs 1/2 for **4**) is also striking. We propose that the α-Me Cp substituents in **7** disfavor the lateral deformation which would stabilize the *meso* isomer.

Influence of $Zr(NR_2)_4$ Steric Properties on Amine Elimination Reactivity with 6. One potential advantage of the amine elimination over the salt elimination route to *ansa*-zirconocene compounds is the possibility of controlling reactivity and stereoselectivity via adjustment of the amide steric properties. Accordingly, we have investigated reactivity of **6** with a series of $Zr(NR_2)_4$ compounds (eq 4).

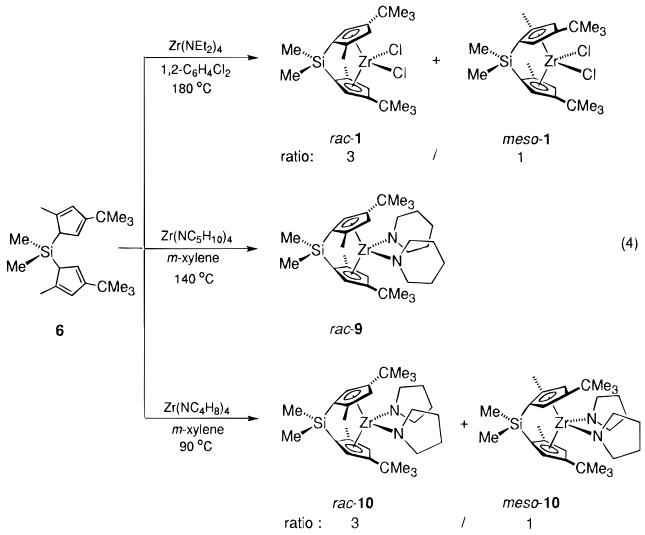

The reaction of **6** with $Zr(NEt_2)_4$ was studied under a variety of conditions. Compound **6** does not react with $Zr(NEt_2)_4$ in *m*-xylene at 140 °C for 14 h (open system) or in mesitylene at 160 °C for 18 h (open system). Thus the greater steric bulk of $-NEt_2$ versus $-NMe_2$ dramatically inhibits the amine elimination reaction with **6** (compare to eq 3). However, when the reaction of **6**

(20) Denninger, U.; Stern, C. L.; Marks, T. J. *Abstracts of Papers*, 208th National Meeting of the American Chemical Society, Washington, DC, 1994; American Chemical Society: Washington, DC, 1994; INOR 527.

(21) (a) Similar results are obtained in other solvents. The reaction of **6** and $Zr(NMe_2)_4$ in *m*-xylene at 140 °C for 3 h yields **7** (90% NMR) in a *rac*/*meso* ratio of 2.5/1. In chlorobenzene at 125 °C, the reaction is complete in less than 3 h and a *rac*-**7**/*meso*-**7** ratio of 2.5/1 is obtained. At 90 °C in chlorobenzene, the reaction is complete in less than 3 h and a *rac*-**7**/*meso*-**7** ratio of 3.0/1 is obtained. (b) Bubbling N_2 through the reaction mixture (toluene, 100 °C), to more rapidly remove the volatile NMe_2H coproduct from the reaction vessel, had no effect on the stereoselectivity. This is in contrast to the kinetic *rac*/*meso* ratio of 1/1 obtained for (EBI)$Zr(NMe_2)_2$ under such N_2 purge conditions and suggests that the isomerization of **7** is much faster than that of (EBI)$Zr(NMe_2)_2$.

and $Zr(NEt_2)_4$ was performed in 1,2-dichlorobenzene at 180 °C (20 h, system open to oil bubbler), $Me_2Si(1\text{-}C_5H_2\text{-}2\text{-}Me\text{-}4\text{-}^tBu)_2ZrCl_2$ (**1**) was formed in 35% NMR yield with a *rac*/*meso* ratio of 3/1, along with unreacted **6** and insoluble decomposition products. Thus, under these forcing conditions, metallocene formation occurs and the solvent acts as a chlorinating agent. We previously reported that the reaction of $Zr(NEt_2)_4$ and $(EBI)H_2$ in 1,2-dichlorobenzene at 180 °C affords $(EBI)ZrCl_2$.[10,22]

Steric crowding in the piperidide complex $Zr(NC_5H_{10})_4$ is expected to be intermediate between that in $Zr(NMe_2)_4$ and $Zr(NEt_2)_4$, because the CH_2 groups of the piperidide ligand are tied back in a six-membered ring. The reaction of **6** with $Zr(NC_5H_{10})_4$ in *m*-xylene at 100 °C for 6 h, with a flow of N_2 bubbling through the reaction solution to help sweep away the piperidine coproduct, results in less than 5% conversion to *rac*-$Me_2Si(1\text{-}C_5H_2\text{-}2\text{-}Me\text{-}4\text{-}^tBu)_2Zr(NC_5H_{10})_2$ (*rac*-**9**); the *meso* isomer of **9** was not observed. However, at higher temperatures (140 °C, 24 h, system open to oil bubbler), this reaction afforded *rac*-**9** in 35% NMR yield, again with no *meso*-**9** detected. Longer reaction times do not result in an increased yield of **9** due to competitive thermal decomposition reactions.[23,24] Recrystallization from Et_2O afforded pure *rac*-**9**, a yellow crystalline solid, in 7% isolated yield. Thus $Zr(NC_5H_{10})_4$ is also much less reactive with **6** than is $Zr(NMe_2)_4$.

In contrast, the pyrrolidide complex $Zr(NC_4H_8)_4$, in which the CH_2 groups of the amides are tied back in a five-membered ring, reacts with **6** under milder conditions. The reaction of $Zr(NC_4H_8)_4$ and **6** in *m*-xylene at 90 °C for 4 h, with a flow of N_2 bubbling through the reaction solution to sweep away the pyrrolidine coproduct, affords $Me_2Si(1\text{-}C_5H_2\text{-}2\text{-}Me\text{-}4\text{-}^tBu)_2Zr(NC_4H_8)_2$ (**10**) in 80% NMR yield with a *rac*/*meso* ratio of 3/1. Recrystallization from hexane affords pure *rac*-**10**, a yellow crystalline solid, in 39% yield.

The qualitative rate trend for metallocene formation in the reactions of **6** with $Zr(NR_2)_4$ compounds is thus $Zr(NMe_2)_4$, $Zr(NC_4H_8)_4 > Zr(NC_5H_{10})_4 > Zr(NEt_2)_4$. Clearly steric crowding in the amide reactant hinders the amine elimination. Note that as pyrrolidine (HNC_4H_8, bp = 87 °C) and piperidine (HNC_5H_{10}, bp 106 °C) are less volatile than NEt_2H (bp 55 °C), the volatility of the amine coproduct (i.e. the ease of removal of amine from the system) is not the limiting factor in these reactions. In contrast, the *rac*/*meso* product ratio increases with increasing amide steric bulk; i.e. the *rac*/*meso* ratio trend is **9** (no *meso* isomer detected) > **7** (*rac*/*meso* = 2.5/1), **10** (*rac*/*meso* = 3/1).

Molecular Structure of *rac*-$Me_2Si(1\text{-}C_5H_2\text{-}2\text{-}Me\text{-}4\text{-}tBu)_2Zr(NC_4H_8)_2$ (*rac*-10). As steric factors strongly influence the reactivity and stereoselectivity in amine elimination syntheses of *ansa*-zirconocene bis(amide) complexes, the molecular structures of such complexes are of interest. The molecular structure of bis(pyrrolidide) complex *rac*-**10** was determined by single-crystal X-ray diffraction (Figure 1, Tables 1 and 2). The monomeric, *ansa*-bridged, bent metallocene structure of *rac*-**10** is similar to that of the dichloride analogue *rac*-**1**,[5] but exhibits significant distortions due to steric crowding between the amide ligands and the Cp substituents. For *rac*-**10** the centroid−Zr−centroid angle is smaller (122.5°), the N−Zr−N angle (99.6°) is larger, and the average Zr−centroid distance is longer (2.35 Å) than the analogous values in *rac*-**1** (cent−Zr−cent 126.7°, Cl−Zr−Cl 97.6°, Zr−cent 2.23 Å), due to the greater size of the amide versus the chloride ligands. The stronger electron-donating ability of pyrrolidide relative to chloride may also contribute to the longer Zr−Cp distance in *rac*-**10** versus *rac*-**1**.

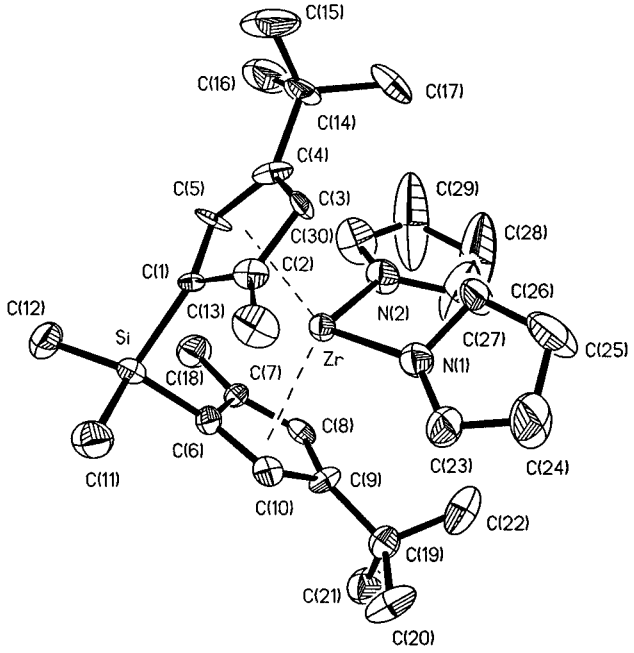

Figure 1. Molecular structure of *rac*-$Me_2Si(1\text{-}C_5H_2\text{-}2\text{-}Me\text{-}4\text{-}^tBu)_2Zr(NC_4H_8)_2$ (*rac*-**10**).

Table 1. Crystallographic Data for *rac*-$Me_2Si(1\text{-}C_5H_2\text{-}2\text{-}Me\text{-}4\text{-}^tBu)_2Zr(NC_4H_8)_2$ (*rac*-10)

empirical formula	$C_{30}H_{50}N_2SiZr$
fw	558.03
temp	295(2) K
wavelength	0.710 73 Å
cryst system	triclinic
space group	$P\bar{1}$
unit cell dimens	a = 10.625(2) Å, α = 75.92(3)°; b = 11.112(3) Å, β = 73.99(1)°; c = 14.902(2) Å, γ = 63.64(3)°
V	1500.3(5) Å3
Z	2
D(calcd)	1.235 g/cm^3
abs coeff	4.26 cm^{-1}
F(000)	596
cryst size	0.10 × 0.08 × 0/20 mm
θ range for data collcn	2.07−19.99°
index ranges	$-1 \le h \le 9$, $-9 \le k \le 10$, $-14 \le l \le 14$
reflcns collcd	3367
indepdt reflcns	2762 (R_{int} = 0.0761)
refinement method	full-matrix least squares on F^2
data/restraints/params	2410/0/317
goodness-of-fit on F^2	0.997
final R indices [$I > 2\sigma(I)$]	$R1$ = 0.0763, w$R2$ = 0.1536
R indices (all data)	$R1$ = 0.1551, w$R2$ = 0.1944
largest diff peak and hole	0.482 and −0.499 e Å^{-3}

(22) Similarly, the reaction of $Zr(NMe_2)_4$ with the N_4-macrocycle $(Me_4taen)H_2$ yields $(Me_4taen)Zr(NMe_2)_2$ when performed in pentane and the dichloride derivative $(Me_4taen)ZrCl_2(NMe_2H)$ when performed in CH_2Cl_2: Black, D. G.; Swenson, D. C.; Jordan, R. F.; Rogers, R. D. *Organometallics* **1995**, *14*, 3539.

(23) One likely mechanism for thermal decomposition of Zr amide complexes is cyclometalation. Labeling studies by Nugent provide evidence for facile metalation of NMe_2 ligands of $Zr(NMe_2)_4$ at elevated temperatures: Nugent, W. A.; Ovenall, D. W.; Holmes, S. J. *Organometallics* **1983**, *2*, 161.

(24) Similar results were obtained in refluxing chlorobenzene (30% conversion to *rac*-**9** after 17 h, no N_2 purge). The use of refluxing 1,2-dichloroethane resulted mainly in decomposition.

Table 2. Selected Bond Lengths (Å) and Angles (deg) for *rac*-$Me_2Si(1\text{-}C_5H_2\text{-}2\text{-}Me\text{-}4\text{-}^tBu_2Zr(NC_4H_8)_2$ (*rac*-10)

Zr−N(1)	2.033(12)	Zr−N(2)	2.084(11)
Zr−C(1)	2.551(12)	Zr−C(2)	2.561(12)
Zr−C(3)	2.720(13)	Zr−C(4)	2.778(13)
Zr−C(5)	2.594(14)	Zr−C(6)	2.541(13)
Zr−C(7)	2.546(14)	Zr−C(8)	2.690(13)
Zr−C(9)	2.772(13)	Zr−C(10)	2.595(13)
Zr−Cp(1)[a]	2.357	Zr−Cp(2)[a]	2.348
Si−C(1)	1.832(12)	Si−C(6)	1.833(14)
Si−C(11)	1.855(14)	Si−C(12)	1.846(14)
N(1)−C(23)	1.47(2)	N(2)−C(27)	1.45(2)
N(1)−C(26)	1.47(2)	N(2)−C(30)	1.45(2)
N(1)−Zr−N(2)	99.6(5)	Cp(1)−Zr−Cp(2)[a]	122.5
C(1)−Si−C(6)	97.1(6)	C(1)−Si−C(11)	115.4(7)
C(23)−N(1)−C(26)	98.1(12)	C(27)−N(2)−C(30)	103.4(13)
C(23)−N(1)−Z	141.6(10)	C(30)−N(2)−Zr	131.0(11)
C(26)−N(1)−Zr	118.4(10)	C(27)−N(2)−Zr	123.4(10)

[a] Cp(1) and Cp(2) are the centroids of the C(1)−C(5) and C(6)−C(10) cycopentadienyl rings.

The structure of *rac*-**10** shows significant lateral deformation. The dihedral angle between centroid−Si−centroid and centroid−Zr−centroid planes is 9.2°, compared to 0° for *rac*-**1**. The presence of significant lateral deformation in *rac*-**10**, despite the α-Me substituents and the *rac* structure, is indicative of severe steric crowding between the NC_4H_8 and ^{t}Bu groups. Steric interactions between these groups are manifested by other structural distortions.[25] The β-^{t}Bu groups of *rac*-**10** are bent 12.0° (C(14)) and 13.2° (C(19)) out of the Cp ring planes, compared with 10° for *rac*-**1**. Similarly the α-Me groups of *rac*-**10** are bent 6.0° (C(13)) and 7.6° (C(18)) out of the Cp ring planes, compared with less than 1° for *rac*-**1**. The N−Zr−N plane of *rac*-**10** is "skewed" 7.1° relative to the Me−Si−Me plane, compared with 9° for the Cl−Zr−Cl/Me−Si−Me planes of *rac*-**1**.

The Zr−N(1) and Zr−N(2) bond lengths (2.03 and 2.08 Å) of *rac*-**10** are similar to the Zr−N bond lengths in *rac*-(EBI)$Zr(NMe_2)_2$ (2.06 Å average) and are in the range observed for other unsaturated Zr(IV) amide complexes (2.00−2.17 Å).[26] The amide groups of *rac*-**10** are nearly flat (sum of angles around N(1) = 358.1°, N(2) = 357.8°). The dihedral angles between the N−Zr−N plane and the amide C−N−C planes of *rac*-**10** are 48.2° for N(1) and 19.1° for N(2); thus, the amide ligands are twisted far (42 and 71°, respectively) from the perpendicular orientation which is optimum for Zr−N π-bonding.[27] The amide with the orientation closest to that optimum for Zr−N π-bonding (N(1)) also has the shorter Zr−N bond length. These data are consistent with sp^2 hybridization at N and partial N to Zr π-donation. Steric crowding between the NC_4H_8 and ^{t}Bu groups in *rac*-**10** prevents the amides from adopting a more perpendicular orientation. The molecular structure of *rac*-(EBI)$Zr(NMe_2)_2$ showed similar evidence for partial M−N π-bonding.[8b] The Zr−N bond lengths for the pyrrolidide (NC_4H_8) ligands in *rac*-**10** (2.06 Å average) are significantly shorter than Zr−N bond lengths for the unsaturated pyrrolide (NC_4H_4) ligands in $Cp_2Zr(NC_4H_4)_2$ (2.17 Å average);[26e] this difference reflects the involvement of the N pπ electrons in the NC_4H_4 ring aromaticity and hence reduced N to Zr π-donation in $Cp_2Zr(NC_4H_4)_2$.

Steric crowding in the piperidide complex **9** and the diethylamide complex $Me_2Si(1\text{-}C_5H_2\text{-}2\text{-}Me\text{-}4\text{-}^tBu)_2Zr(NEt_2)_2$ (not observed), which contain larger amide ligands, must be more severe than in *rac*-**10**, which may contribute to the low yields in these cases.

Conversion of *rac*-$Me_2Si(1\text{-}C_5H_2\text{-}2\text{-}Me\text{-}4\text{-}^tBu)_2Zr(NR_2)_2$ to *rac*-1. *rac*-$Me_2Si(1\text{-}C_5H_2\text{-}2\text{-}Me\text{-}4\text{-}^tBu)_2Zr(NR_2)_2$ complexes can be cleanly converted the dichloride complex *rac*-**1** by reaction with Me_3SiCl (eq 5). The

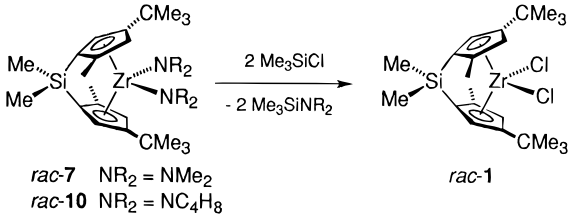

(5)

reaction of *rac*-**7** with excess (5 equiv) Me_3SiCl in C_6D_6 at 23 °C was monitored by ^{1}H NMR spectroscopy which showed the formation of *rac*-**1** (80%) and *rac*-$Me_2Si(1\text{-}C_5H_2\text{-}2\text{-}Me\text{-}4\text{-}^tBu)_2Zr(NMe_2)Cl$ (**11**, 20%) after 75 min and complete conversion to *rac*-**1** plus 2 equiv of Me_3SiNMe_2 after 4 h. Similarly, the reaction of pyrrolidide complex *rac*-**10** with excess (5 equiv) Me_3SiCl in C_6D_6 at 23 °C yields rac-**1** (100%) plus 2 equiv of $Me_3SiNC_4H_8$ in less than 1 h.

Summary

Me_2Si-bridged *ansa*-zirconocene complexes of interest for α-olefin polymerization catalysis can be prepared in good yield by amine elimination. The reaction of $Me_2Si(C_5H_4\text{-}3\text{-}^tBu)_2$ (**3**) and $Zr(NMe_2)_4$ affords $Me_2Si(1\text{-}C_5H_3\text{-}3\text{-}^tBu)_2Zr(NMe_2)_2$ (**4**) in 95% NMR yield (*rac*/*meso* ratio = 1/2) and pure *meso*-**4** in 38% isolated yield. The introduction of α-Me Cp substituents improves the *rac*/*meso* product ratio significantly. The reaction of $Me_2Si(1\text{-}C_5H_3\text{-}2\text{-}Me\text{-}4\text{-}^tBu)_2$ (**6**) with $Zr(NMe_2)_4$ affords $Me_2Si(1\text{-}C_5H_2\text{-}2\text{-}Me\text{-}4\text{-}^tBu)_2Zr(NMe_2)_2$ (**7**) in 90% NMR yield (*rac*/*meso* product ratio = 2.5/1) and pure *rac*-**7** in 52% isolated yield. The *rac*/*meso* ratios obtained for **4** and **7** are thermodynamic ratios, and the *rac*/*meso* isomerizations are catalyzed by NMe_2H. The isomerization reactions of **4** and **6** are analogous to that of (EBI)$Zr(NMe_2)_2$ and proceed by reversible aminolysis of the Zr−Cp bonds to form mono(cyclopentadienyl) zirconium tris(amide) intermediate species (Scheme 1). The thermodynamic preference for the *meso* diastereomer of **4** may reflect the relief of steric crowding in this species by a lateral deformation distortion. A higher thermodynamic *rac*/*meso* ratio is observed for **7** because the

(25) Several close H−H contacts (<2.0 Å) are observed between the ^{t}Bu and pyrolidide hydrogens (H_{30B}/H_{16A}, H_{23B}/H_{20B}) of *rac*-**10**.

(26) Representative Zr(IV) amide complexes and average Zr−N distances: (a) $Zr(NMe_2)_4$, 2.07 Å (electron diffraction). Hagen, K.; Holwill, C. J.; Rice, D. A.; Runnacles, J. D. *Inorg. Chem.* **1988**, *27*, 2032. (b) $(Me_2N)_3Zr(\mu\text{-}NMe_2)_2Zr(NMe_2)_3$, terminal Zr−N 2.04−2.11 Å. Chisholm, M. H.; Hammond, C. E.; Huffman, J. C. *Polyhedron* **1988**, *7*, 2515. (c) $(Me_2N)_2Zr(\mu\text{-}N^tBu)_2Zr(NMe_2)_2$, 2.06 Å. Nugent, W. A.; Harlow, R. L. *Inorg. Chem.* **1979**, *18*, 2030. (d) *rac*-$Me_2Si(\eta^5\text{-}C_9H_6)_2Zr(NMe_2)_2$, 2.07 Å; ref 11. (e) $Cp_2Zr(NC_4H_4)_2$, 2.17 Å. Bynum, R. V.; Hunter, W. E.; Rogers, R. D.; Atwood, J. L. *Inorg. Chem.* **1980**, *19*, 2368. (f) $Zr(\eta^5,\eta^1\text{-}C_5H_4SiMe_2NPh)$, 2.13 Å. Herrmann, W. A.; Morawietz, M. J. A.; Priermeier, T. *Angew. Chem., Int. Ed. Engl.* **1994**, *33*, 1946. (g) $Cp^*Zr(NPr^i_2)Cl_2$, 2.00 Å. Pupi, R. M.; Coalter, J. N.; Petersen, J. L. *J. Organomet. Chem.* **1995**, *497*, 17. (h) $(\eta^5\text{-}C_2B_9H_{11})Zr(NEt_2)_2(NHEt_2)$, $Zr-NEt_2$ = 2.04 Å, $Zr-NHEt_2$ = 2.36 Å. Bowen, D. E.; Jordan, R. F.; Rogers, R. D. *Organometallics* **1995**, *14*, 3630. (i) $(Me_4taen)Zr(NMe_2)_2$, 2.11 Å; ref 22.

(27) Lauher, J. W.; Hoffmann, R. *J. Am. Chem. Soc.* **1976**, *98*, 1729.

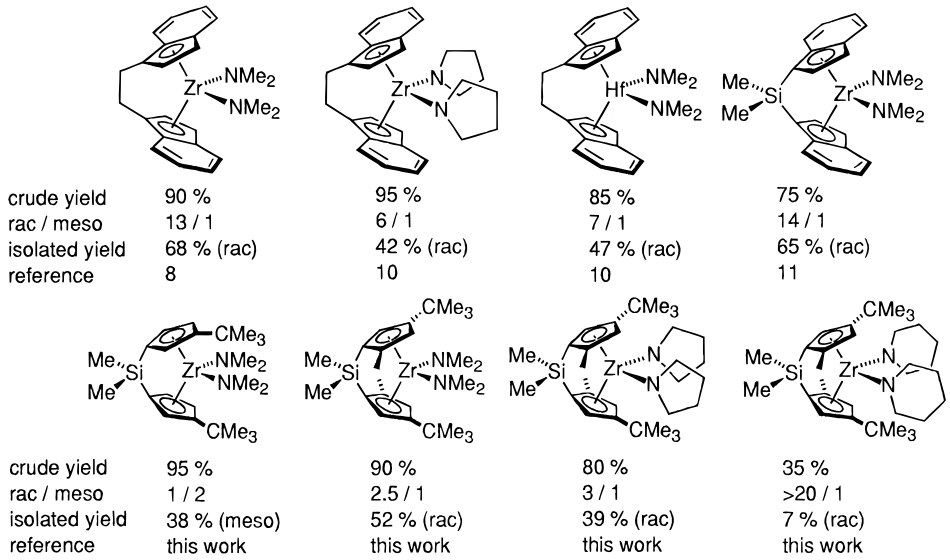

Figure 2. Summary of chiral *ansa*-metallocenes prepared by amine elimination. Crude yields were detrmined by NMR. The *rac*/*meso* ratios are those for the crude products. Isolated yields listed are recrystallized yields of the pure isomer indicated.

α-Me Cp substituents in *meso*-**7** disfavor the lateral deformation.

Steric crowding in $Zr(NR_2)_4$ amide compounds inhibits the amine elimination reaction with $Me_2Si(1\text{-}C_5H_3\text{-}2\text{-}Me\text{-}4\text{-}^tBu)_2$ (**6**). The qualitative rate trend for metallocene formation in the reactions of **6** with $Zr(NR_2)_4$ compounds is $Zr(NMe_2)_4$, $Zr(NC_4H_8)_4 > Zr(NC_5H_{10})_4 > Zr(NEt_2)_4$. The reaction of **6** with $Zr(NMe_2)_4$ proceeds readily in toluene at 100 °C (5 h) and provides pure *rac*-**7** in 52% isolated yield. *rac*-**7** is cleanly and stereospecifically converted to *rac*-$Me_2Si(1\text{-}C_5H_2\text{-}2\text{-}Me\text{-}4\text{-}^tBu)_2ZrCl_2$ (*rac*-**1**) via reaction with Me_3SiCl. This synthesis of *rac*-$Me_2Si(1\text{-}C_5H_2\text{-}2\text{-}Me\text{-}4\text{-}^tBu)_2ZrX_2$ zirconocenes is a significant improvement over the salt elimination synthesis.[5] In contrast, the reaction of **6** with $Zr(NEt_2)_4$ yields a metallocene product, *rac*-$Me_2Si(1\text{-}C_5H_2\text{-}2\text{-}Me\text{-}4\text{-}^tBu)_2ZrCl_2$ (*rac*-**1**), only under forcing conditions (1,2-dichlorobenzene, 180 °C) where solvent participation occurs.

The use of bulky amide ligands does increase the *rac*/*meso* product ratios in amine elimination reactions of **6** and $Zr(NR_2)_4$ compounds. The *rac*/*meso* ratio trend is **9** (no *meso* isomer detected) > **7** (*rac*/*meso* = 2.5/1), **10** (*rac*/*meso* = 3/1). Due to the opposite effects of amide steric bulk on reactivity and stereoselectivity, $Zr(NMe_2)_4$ is the optimum starting material for the synthesis of *rac*-$Me_2Si(1\text{-}C_5H_2\text{-}2\text{-}Me\text{-}4\text{-}^tBu)_2ZrX_2$ complexes via amine elimination.

In conclusion, in this paper and in others in this series, we have shown that a wide variety of chiral *ansa*-metallocene complexes can be prepared via amine elimination chemistry.[8−11] A summary of the *ansa*-metallocenes prepared, together with the yields and stereoselectivities, is provided in Figure 2. In many cases, the amine elimination reactions offer an attractive alternative to the current salt elimination syntheses.

Experimental Section

General Procedures. All reactions were performed under a purified N_2 atmosphere using standard glovebox and Schlenk techniques. Solvents were distilled from Na/benzophenone, except for toluene (Na) and chlorinated solvents (CaH_2), and stored under N_2. $Me_2Si(1\text{-}C_5H_4\text{-}3\text{-}^tBu)_2$ (**3**) and $Me_2Si(1\text{-}C_5H_3\text{-}2\text{-}Me\text{-}4\text{-}^tBu)_2$ (**6**) were prepared by the literature procedures.[5] $Zr(NMe_2)_4$, $Zr(NEt_2)_4$, and $Zr(NC_4H_8)_4$ were prepared using modifications of the original Bradley procedure,[28] as described in earlier papers in this series.[8,10] NMR spectra were recorded on a Bruker AMX-360 spectrometer, in Teflon-valved or flame-sealed tubes, at ambient probe temperature unless otherwise indicated. ^1H and ^{13}C chemical shifts are reported versus Me_4Si and were determined by reference to the residual ^1H and ^{13}C solvent peaks. Elemental analyses were performed by E + R Microanalytical Laboratory (Corona, NY).

***meso*-$Me_2Si(1\text{-}C_5H_3\text{-}3\text{-}^tBu)_2Zr(NMe_2)_2$ (*meso*-4).** A toluene (10 mL) solution of $Me_2Si(1\text{-}C_5H_4\text{-}3\text{-}^tBu)_2$ (**3**, 0.29 g, 0.98 mmol) was added to a toluene (5 mL) solution of $Zr(NMe_2)_4$ (0.27 g, 1.0 mmol). The reaction mixture was stirred and heated to 100 °C for 17 h, and evolved NMe_2H was allowed to escape via an oil bubbler. The solvent was removed under reduced pressure affording an oily yellow solid. The ^1H NMR spectrum of the crude product showed that $Me_2Si(1\text{-}C_5H_3\text{-}3\text{-}^tBu)_2Zr(NMe_2)_2$ (**4**) was present in 95% NMR yield in a *rac*/*meso* ratio of 1/2. The crude product was recrystallized from hexane, affording pure *meso*-**4** in 38% yield (0.18 g) as a yellow crystalline solid. Anal. Calcd for $C_{24}H_{42}N_2SiZr$: C, 60.31; H, 8.86; N, 5.86. Found: C, 60.31; H, 9.05; N, 5.62. ^1H NMR (C_6D_6): δ 6.66 (dd, J = 3 Hz, J = 2 Hz, 2 H, C_5H_3), 5.91 (pseudo t, J = 2 Hz, 2 H, C_5H_3), 5.42 (pseudo t, J = 3 Hz, 2 H, C_5H_3), 2.90 (s, 6 H, NMe_2), 2.54 (s, 6 H, NMe_2), 1.28 (s, 18 H, ^{t}Bu), 0.54 (s, 3 H, Si−CH_3), 0.49 (s, 3 H, Si-CH_3). $^{13}C\{^1H\}$ NMR (C_6D_6): δ 144.9 (C), 119.2 (CH), 111.6 (CH), 107.3 (CH), 107.1 (C), 50.7 (NMe_2), 46.9 (NMe_2), 32.9 ($C(CH_3)_3$), 31.8 ($C(CH_3)_3$), −2.3 (Si-CH_3), −5.7 (Si-CH_3).

***rac*-$Me_2Si(1\text{-}C_5H_3\text{-}3\text{-}^tBu)_2Zr(NMe_2)_2$ (*rac*-4).** This species was characterized by ^1H NMR spectroscopy only. ^1H NMR (C_6D_6): δ 6.47 (dd, J = 3 Hz, J = 2 Hz, 2 H, C_5H_3), 5.79 (pseudo t, J = 2 Hz, 2 H, C_5H_3), 5.67 (pseudo t, J = 3 Hz, 2 H, C_5H_3), 2.61 (s, 12 H, NMe_2), 1.30 (s, 18 H, ^{t}Bu), 0.49 (s, 6 H, $SiMe_2$).

***rac*-$Me_2Si(1\text{-}C_5H_2\text{-}2\text{-}Me\text{-}4\text{-}^tBu)_2Zr(NMe_2)_2$ (*rac*-7).** A Schlenk vessel was charged with $Zr(NMe_2)_4$ (0.93 g, 3.5 mmol), $Me_2Si(1\text{-}C_5H_3\text{-}2\text{-}Me\text{-}4\text{-}^tBu)_2$ (**6**, 1.0 g, 3.0 mmol), and toluene (25 mL). The reaction mixture was stirred and heated to 100 °C for 5 h, and NMe_2H was allowed to escape via an oil

(28) (a) Bradley, D. C.; Thomas, I. M. *Proc. Chem. Soc.* **1959**, 225. (b) Bradley, D. C.; Thomas, I. M. *J. Chem. Soc.* **1960**, 3857.

bubbler. An aliquot was removed and analyzed by ^{1}H NMR, which showed that $Me_2Si(1\text{-}C_5H_2\text{-}2\text{-}Me\text{-}4\text{-}^tBu)_2Zr(NMe_2)_2$ (**7**) was present in 90% NMR yield in a *rac*/*meso* ratio of 2.5/1. The volatiles were removed under reduced pressure and the crude product was recrystallized from hexane, yielding pure *rac*-**7** in 52% yield (0.80 g) as a yellow crystalline solid. Anal. Calcd for $C_{26}H_{46}N_2SiZr$: C, 61.72; H, 9.16; N, 5.54. Found: C, 61.67; H, 9.25; N, 5.40. ^{1}H NMR (C_6D_6): δ 6.27 (d, J = 2 Hz, 2 H, C_5H_2), 5.57 (d, J = 2 Hz, 2 H, C_5H_2), 2.70 (s, 12 H, NMe_2), 2.06 (s, 6 H, Me), 1.34 (s, 18 H, ^{t}Bu), 0.57 (s, 6 H, $SiMe_2$). $^{13}C\{^1H\}$ NMR (C_6D_6): δ 147.7 (C), 126.0 (C), 115.0 (CH), 106.1 (CH), 106.0 (C), 49.3 (NMe_2), 33.3 ($C(CH_3)_3$), 32.0 ($C(CH_3)_3$), 17.0 (CH_3), −0.8 ($SiMe_2$).

***meso*-$Me_2Si(1\text{-}C_5H_2\text{-}2\text{-}Me\text{-}4\text{-}^tBu)_2Zr(NMe_2)_2$ (*meso*-7).** This species was characterized by ^{1}H NMR spectroscopy only. ^{1}H NMR (C_6D_6): δ 6.35 (d, J = 2 Hz, 2 H, C_5H_2), 5.54 (d, J = 2 Hz, 2 H, C_5H_2), 3.05 (s, 6 H, NMe_2), 2.62 (s, 6 H, NMe_2), 2.07 (s, 6 H, Me), 1.28 (s, 18 H, ^{t}Bu), 0.63 (s, 3 H, Si−CH_3), 0.53 (s, 3 H, Si−CH_3).

Reaction of $Me_2Si(1\text{-}C_5H_3\text{-}2\text{-}Me\text{-}4\text{-}^tBu)_2$ (6) with $Zr(NEt_2)_4$. A mixture of $Zr(NEt_2)_4$ (0.10 g, 0.28 mmol) and $Me_2Si(1\text{-}C_5H_3\text{-}2\text{-}Me\text{-}4\text{-}^tBu)_2$ (**6**, 0.091 g, 0.28 mmol) in 1,2-dichlorobenzene (10 mL) was stirred and heated to 180 °C for 20 h, with the reaction vessel open to an oil bubbler. The volatiles were removed under reduced pressure and analyzed by ^{1}H NMR, which showed that the product mixture contained 35% $Me_2Si(1\text{-}C_5H_2\text{-}2\text{-}Me\text{-}4\text{-}^tBu)_2ZrCl_2$ (**1**) in a *rac*/*meso* ratio of 3/1 and 65% unreacted **6**, along with insoluble decomposition products.

$Zr(NC_5H_{10})_4$. In a modification of Bradley's original procedure,[28] piperidine ($C_5H_{10}NH$, 12 g, 140 mmol) was added to a Schlenk vessel containing $Zr(NMe_2)_4$ (1.5 g, 5.6 mmol). The vessel was fitted with a condenser and an oil bubbler, and the reaction mixture was stirred and refluxed for 17 h. An aliquot was removed and analyzed by ^{1}H NMR which showed complete conversion to $Zr(NC_5H_{10})_4$. The volatiles were removed under reduced pressure yielding a pale yellow solid which was dried under vacuum overnight. Yield of $Zr(NC_5H_{10})_4$: 2.0 g (81%). ^{1}H NMR (C_6D_6): δ 3.49 (m, 16 H, NCH_2), 1.49 (m, 24 H, CH_2). $^{13}C\{^1H\}$ NMR (C_6D_6): δ 50.8 (NCH_2), 29.6 (CH_2), 26.1 (CH_2).

***rac*-$Me_2Si(1\text{-}C_5H_2\text{-}2\text{-}Me\text{-}4\text{-}^tBu)_2Zr(NC_5H_{10})_2$ (*rac*-9).** A *m*-xylene (30 mL) solution of $Me_2Si(1\text{-}C_5H_3\text{-}2\text{-}Me\text{-}4\text{-}^tBu)_2$ (**6**, 0.33 g, 1.0 mmol) and $Zr(NC_5H_{10})_4$ (0.43 g, 1.0 mmol) was stirred and heated to 140 °C for 23 h, while open to an oil bubbler. An aliquot was removed and analyzed by ^{1}H NMR which showed the presence of 65% starting materials and 35% *rac*-$Me_2Si(1\text{-}C_5H_2\text{-}2\text{-}Me\text{-}4\text{-}^tBu)_2Zr(NC_5H_{10})_2$ (*rac*-**9**) and no *meso*-**9**. The volatiles were removed under reduced pressure and the crude product was recrystallized from Et_2O, yielding pure *rac*-**9** as a yellow crystalline solid (40 mg, 7%). Anal. Calcd for $C_{32}H_{54}N_2SiZr$: C, 65.57; H, 9.29; N, 4.78. Found: C, 65.36; H, 9.36; N, 4.50. ^{1}H NMR (C_6D_6): δ 6.46 (d, J = 2 Hz, 2 H, C_5H_2), 5.48 (d, J = 2 Hz, 2 H, C_5H_2), 3.11 (m, 4 H, NCH_2), 3.04 (m, 4 H, NCH_2), 2.06 (s, 6 H, Me), 1.61 (m, 4 H, CH_2), 1.56 (m, 4 H, CH_2), 1.44 (s, 18 H, ^{t}Bu), 1.37 (m, 4 H, CH_2), 0.57 (s, 6 H, $SiMe_2$). $^{13}C\{^1H\}$ NMR (C_6D_6): δ 148.6 (C), 125.3 (C), 114.7 (CH), 104.9 (C), 103.8 (CH), 57.4 (NCH_2), 33.7 ($C(CH_3)_3$), 32.2 ($C(CH_3)_3$), 28.0 (CH_2), 25.9 (CH_2), 17.2 (CH_3), −0.8 ($SiMe_2$).

***rac*-$Me_2Si(1\text{-}C_5H_2\text{-}2\text{-}Me\text{-}4\text{-}^tBu)_2Zr(NC_4H_8)_2$ (*rac*-10).** A *m*-xylene (12 mL) solution of $Me_2Si(1\text{-}C_5H_3\text{-}2\text{-}Me\text{-}4\text{-}^tBu)_2$ (**6**, 0.33 g, 1.0 mmol) was added to a *m*-xylene (12 mL) solution of $Zr(NC_4H_8)_4$ (0.38 g, 1.0 mmol). The reaction mixture was stirred and heated to 90 °C for 4 h, with a flow of N_2 bubbling through the reaction mixture to sweep away the pyrrolidine coproduct. An aliquot was removed and analyzed by ^{1}H NMR which showed that $Me_2Si(1\text{-}C_5H_2\text{-}2\text{-}Me\text{-}4\text{-}^tBu)_2Zr(NC_4H_8)_2$ (**10**) was present in 80% NMR yield in a *rac*/*meso* ratio of 3/1. The volatiles were removed under reduced pressure and the crude product was recrystallized from hexane, yielding pure *rac*-**10** in 39% yield (0.22 g) as a yellow crystalline solid. Anal. Calcd for $C_{30}H_{50}N_2SiZr$: C, 64.57; H, 9.03; N, 5.02. Found: C, 64.66; H, 9.23; N, 4.91. ^{1}H NMR (C_6D_6): δ 6.18 (d, J = 2 Hz, 2 H, C_5H_2), 5.71 (d, J = 2 Hz, 2 H, C_5H_2), 3.30 (m, 4 H, NCH_2), 3.21 (m, 4 H, NCH_2), 2.12 (s, 6 H, Me), 1.60 (m, 4 H, CH_2), 1.49 (m, 4 H, CH_2), 1.33 (s, 18 H, ^{t}Bu), 0.57 (s, 6 H, $SiMe_2$). $^{13}C\{^1H\}$ NMR (C_6D_6): δ 147.8 (C), 126.1 (C), 116.0 (CH), 105.9 (C), 105.8 (CH), 56.8 (NCH_2), 33.1 ($C(CH_3)_3$), 32.0 ($C(CH_3)_3$), 26.1 (CH_2), 16.7 (CH_3), −0.7 ($SiMe_2$).

Reaction of *rac*-$Me_2Si(1\text{-}C_5H_2\text{-}2\text{-}Me\text{-}4\text{-}^tBu)_2Zr(NMe_2)_2$ (*rac*-7) with Me_3SiCl. Excess Me_3SiCl (31 μL, 0.25 mmol) was added via microsyringe to a solution of *rac*-**7** (0.025 g, 0.049 mmol) in C_6D_6 in a Teflon-valved NMR tube, and the tube was agitated to mix the contents. After 4 h at 23 °C ^{1}H NMR showed complete conversion to *rac*-**1** with no detectable epimerization, plus 2 equiv Me_3SiNMe_2, and unreacted Me_3SiCl.

***rac*-1.** ^{1}H NMR (C_6D_6): δ 6.53 (d, J = 2 Hz, 2 H, C_5H_2), 5.47 (d, J = 2 Hz, 2 H, C_5H_2), 1.95 (s, 6 H, Me), 1.40 (s, 18 H, *t*Bu), 0.37 (s, 6 H, $SiMe_2$).

11. ^{1}H NMR (C_6D_6): δ 6.40 (d, J = 2 Hz, 1 H, C_5H_2), 6.03 (d, J = 2 Hz, 1 H, C_5H_2), 5.74 (d, J = 2 Hz, 1 H, C_5H_2), 5.48 (d, J = 2 Hz, 1 H, C_5H_2), 2.80 (s, 6 H, NMe_2), 2.21 (s, 3 H, Me), 2.02 (s, 3 H, Me), 1.45 (s, 9 H, ^{t}Bu), 1.14 (s, 9 H, *t*Bu), 0.49 (s, 3 H, Si-CH_3), 0.40 (s, 3 H, Si-CH_3).

Me_3SiNMe_2. ^{1}H NMR (C_6D_6): δ 2.38 (s, 6 H, NMe_2), 0.05 (s, 9 H, $SiMe_3$).

Reaction of *rac*-$Me_2Si(1\text{-}C_5H_2\text{-}2\text{-}Me\text{-}4\text{-}^tBu)_2Zr(NC_4H_8)_2$ (*rac*-10) with Me_3SiCl. Excess Me_3SiCl (28 μL, 0.22 mmol) was added via microsyringe to a solution of *rac*-**10** (0.025 g, 0.045 mmol) in C_6D_6 in a Teflon-valved NMR tube, and the tube was agitated to mix the contents. After 1 h at 23 °C, ^{1}H NMR spectrum showed complete conversion to *rac*-**1**, with no detectable epimerization, plus 2 equiv $Me_3Si(NC_4H_8)$ and unreacted Me_3SiCl. ^{1}H NMR (C_6D_6) for $Me_3Si(NC_4H_8)$: δ 2.85 (m, 4 H, NCH_2), 1.55 (m, 4 H, CH_2), 0.11 (s, 9 H, $SiMe_3$).

X-ray Diffraction Study of *rac*-$Me_2Si(1\text{-}C_5H_2\text{-}2\text{-}Me\text{-}4\text{-}^tBu)_2Zr(NC_4H_8)_2$ (*rac*-10). The X-ray crystallographic analysis of *rac*-**10** was performed by J.L.P. at WVU. Pertinent crystallographic data are listed in Table 1. Intensity data were measured with graphite-monochromated Mo Kα radiation (χ = 0.710 73 Å) and with ω scans at a fixed rate of 10°/min. Background counts were measured at the beginning and at the end of each scan with the crystal and counter kept stationary. The intensities of three standard reflections were measured periodically during data collection and did not provide any evidence of sample decomposition. The data were corrected for Lorentz−polarization effects. ψ scans were measured, but an empirical absorption correction was not deemed necessary.

The structure solution was initiated with the direct methods structure solution software provided with SHELXTL IRIS. The atom coordinates of the remaining non-hydrogen atoms not located on the initial *E*-map were determined by difference Fourier methods. Following the anisotropic refinement of the non-hydrogen atoms, all hydrogen atom positions were idealized with isotropic temperature factors set at 1.2 times that of the adjacent carbon. The positions of the methyl hydrogens were optimized by a rigid rotating group refinement with idealized tetrahedral angles. The elongated thermal ellipsoids obtained for carbon atoms C(27), C(28), and C(29) are an indication of a conformational disorder. However, due to the limited amount of observed data, attempts to model and refine this disorder were unsuccessful. Full-matrix least-squares refinement,[29] based upon the minimization of $\sum w_i|F_o^2 - F_c^2|^2$, with $w_i^{-1} = [\sigma^2(F_o^2) + (0.0804P)^2]$, where $P = (\max(F_o^2, 0) +$

(29) SHELXL-93 is a FORTRAN-77 program (Professor G. Sheldrick, Institut fur Anorganische Chemie, University of Gottingen, D-37077 Gottingen, Germany) for single-crystal X-ray structural analyses. All computations were performed on a Silicon Graphics Iris Indigo workstation.

$2F_c^2)/3$, converged to give final discrepancy indices[30] of $R1 = 0.0763$, $wR2 = 0.1536$, and GOF = 0.997 for 1593 reflections with $I > 2\sigma(I)$.

Acknowledgment. This work was supported by the National Science Foundation (Grant CHE-9413022; R.F.J.). Several preliminary experiments performed by Katrin Schmidt (visiting graduate student supported by the Stiftung Volkswagen) and Sandra Frantzen (summer undergraduate research student supported by the NSF-REU program) are appreciated.

Supporting Information Available: Text describing X-ray procedures, tables of X-ray data, atom coordinates and thermal parameters, and bond distances and angles, and ORTEP diagrams (12 pages). Ordering information is given on any current masthead page.

OM9601054

(30) The discrepancy indices were calculated from the expressions $R1 = \sum||F_o| - |F_c||/\sum|F_o|$ and $wR2 = [\sum(w_i(F_o^2 - F_c^2)^2)/\sum(w_i(F_o^2)^2]^{1/2}$, and the standard deviation of an observation of unit weight (GOF) is equal to $[\sum(w_i(F_o^2 - F_c^2)^2)/(n - p)]^{1/2}$, where n is the number of reflections and p is the number of parameters varied during the last refinement cycle.